Effect of the Synthesis Method of $MgAl_2O_4$ and of Sn and Pb Addition to Platinum Catalysts on the Behavior in *n*-Butane Dehydrogenation

Sonia Bocanegra,[†] María Julia Yañez,[‡] Osvaldo Scelza,[†] and Sergio de Miguel*,[†]

Instituto de Investigaciones en Catálisis y Petroquímica (INCAPE)/Facultad de Ingeniería Química, Universidad Nacional del Litoral, CONICET, Santiago del Estero 2654, Santa Fe, 3000, Argentina, and CCT-BBca, Centro Científico Tecnológico CONICET, Camino La Carrindanga, Km 7, Bahía Blanca, Argentina

The $MgAl_2O_4$ spinels, synthesized by using two different methods (ceramic and coprecipitation), show very low acidity and good dispersion capacity of the metallic phase, these properties being suitable for the use of these materials as supports. However, $MgAl_2O_4^{cer}$ displays higher strong acidity than $MgAl_2O_4^{cop}$ which seems to influence the metal−support interaction, since $Pt/MgAl_2O_4^{cer}$ catalyst shows higher metallic dispersion, lower metal particle sizes, and better catalytic behavior than the $Pt/MgAl_2O_4^{cop}$ one. The Sn addition to $Pt/MgAl_2O_4$ improves the performance in the *n*-butane dehydrogenation process, increasing the activity, stability, and selectivity to butenes. This behavior is due to the presence of important Pt−Sn interactions, mainly in bimetallic catalysts supported on $MgAl_2O_4^{cer}$. On the other hand, the Pb addition to monometallic catalysts does not enhance the catalytic performance in dehydrogenation. This behavior is in agreement with the characterization results of metallic phase that indicate important blocking effects in $PtPb/MgAl_2O_4^{cer}$ catalysts, and segregation effects in $PtPb/MgAl_2O_4^{cop}$. In conclusion, the ceramic method of $MgAl_2O_4$ preparation provides the best support for PtSn catalysts in *n*-butane dehydrogenation reaction.

Introduction

$MgAl_2O_4$ is used as a catalytic support for different reactions.[1−5] The traditional synthesis to obtain this material is the ceramic method (reaction in solid phase at high temperature). The material obtained by this procedure has certain disadvantages such as low specific surface area and chemical heterogeneity. In order to avoid these problems, other preparation methods have been used: mechanochemical, sol-gel, and coprecipitation.[6−8] With respect to the nature of the metallic phase, it must be indicated that Pt has been intensively used as the active metal, catalyzing several reactions such as hydrogenation, isomerization, dehydrogenation, oxidation of hydrocarbons, etc.[9−11] It can be noted that Pt, compared with other group 8−10 metals, has a high dehydrogenation activity of alkanes and low hydrogenolytic capacity. The performance of the metallic phase could be enhanced by addition of inactive metals of group 14, such as Sn, Pb, and Ge.[3,12,13] It must be remarked that very few papers studied the influence of Pb on the dehydrogenation performance.[14,15] Moreover, no systematic study of the influence of the support preparation on the catalytic behavior of the $MgAl_2O_4$-supported PtPb has been reported.

In this work, two preparation methods of $MgAl_2O_4$ have been used: ceramic and coprecipitation. The supports thus obtained were characterized by measurements of the textural properties (BET isotherms), X-ray diffraction, 2-propanol dehydration reaction, and TPD of pyridine (to determine the acid−base properties). Monometallic catalysts based on Pt and bimetallic catalysts (PtSn and PtPb) were prepared on both supports. These catalysts were characterized by H_2 chemisorption, TEM, TPR, XPS, test reactions of the metallic phase (cyclohexane dehydrogenation and cyclopentane hydrogenolysis) and evaluated in the *n*-butane dehydrogenation reaction in a continuous flow reactor and in a pulse equipment.

* To whom correspondence should be addressed. Tel: 54-342-4555279. Fax: 54-0342- 4531068. E-mail: sdmiguel@fiq.unl.edu.ar.
† Universidad Nacional del Litoral.
‡ Centro Científico Tecnológico CONICET - Bahía Blanca.

The aim of this paper is to compare the effect of the preparation method of the support on the catalytic properties of the PtM (M = Sn or Pb) supported catalysts, and to study the influence of the different amounts of Sn and Pb added to Pt on the characteristics of the metallic phase and on the catalytic performance in *n*-butane dehydrogenation.

Experimental Section

Synthesis of $MgAl_2O_4$. Two preparation methods of $MgAl_2O_4$ were used: (i) ceramic method and (ii) coprecipitation method.

(i). Ceramic Method ($MgAl_2O_4^{cer}$). $MgAl_2O_4$ was prepared by a solid-phase reaction between MgO (Alfa Aesar, purity 99.99%) and γ-Al_2O_3 (CK 300 from Cyanamid Ketjen, purity 99.9%). The steps involved in the preparation of the support were (a) an intimate mixture of the reactants in the stoichiometric ratio (MgO/γ-Al_2O_3 molar ratio = 1), (b) grinding of the mixture to obtain a very fine powder using a mortar (the particle size of the obtained powder was smaller than 105 μm), (c) formation of a paste by addition of distilled water to the powder, (d) drying at 100 °C for 12 h, and (e) calcination in an electric furnace at 900 °C for 24 h. Finally, the solid was ground to particle sizes between 177 and 500 μm (35−80 mesh).

(ii). Coprecipitation Method ($MgAl_2O_4^{cop}$). $Mg(NO_3)_2 \cdot 6H_2O$ (Merck, 99.0% purity), $Al(NO_3)_3 \cdot 9H_2O$ (Merck, 98.5% purity), and ammonia solution (Merck, 28%, analytical grade) were used as reagents. A 0.5 M solution of the nitrates was prepared, with an Al/Mg molar ratio = 2. The precursor was prepared by slowly adding the ammonia solution into the mixed salt solution at 40 °C under stirring until it reached pH = 11. Once the gel is formed, the stirring went on for 10 min. The resulting gel was aged for 1 h at room temperature, and then filtered. Then the gel was washed with distilled water (volumetric ratio = 4:1) under stirring and filtered again. The gel was also washed in the same filter paper with an excess of distilled water, and dried for 24 h at 100 °C. Then, a calcination treatment was performed in air flow (30 mL min^{-1}) at 800 °C

10.1021/ie9009205
Published on Web 03/25/2010

for 4 h. Finally, the solid was ground to particle sizes between 177 and 500 μm (35−80 mesh).

Characterization of $MgAl_2O_4$ Supports. The different stages of preparation of the supports were characterized by X-ray diffraction experiments (XRD), performed at room temperature in a Shimadzu model XD3A instrument using CuK_α radiation (λ =1542 Å), generated at 30 kV and a current of 30 mA .

The specific surface area, pore volume and mean pore radio of both supports were determined through the BET isotherm in a Quantachrome Corporation NOVA-1000 equipment.

In order to characterize the acid properties of the different $MgAl_2O_4$ supports, isopropanol dehydration experiments at atmospheric pressure were carried out in a continuous flow reactor. Prior to the reaction, samples were reduced in situ with H_2 at 500 °C. The alcohol was vaporized in a H_2 stream (H_2/isopropanol molar ratio = 19) and fed to the reactor with a space velocity of 0.52 $mol_{alcohol}\ h^{-1}\ g_{cat}^{-1}$. The sample weight was 100 mg and the reaction temperature was 200 °C. The reactor effluent was analyzed by GC and the only reaction product was propylene.

The measurement of the equilibrium pH of both $MgAl_2O_4$ suspended in water was performed by putting the solid (1 g, 35/80 mesh) in contact with 100 mL of deionized water at room temperature according to the technique reported by Roman-Martinez et al.[16]

The acidity of the supports was also determined by means of temperature-programmed desorption (TPD) of pyridine. An amount of 150 mg of the sample was first immersed in a closed vial containing pure pyridine (Merck, 99.9%) for 4 h. Then the vial was opened and the excess of pyridine was evaporated at room conditions until the surface of the particles was dry. The sample was then loaded into a quartz tube microreactor and supported over a quartz wool plug. A constant flow of nitrogen (40 mL min^{-1}) was passed through the sample. A first step of desorption of weakly adsorbed pyridine and stabilization was performed by heating the sample at 110 °C for 2 h. Then the temperature of the oven was raised to a final value of 550 °C at a heating rate of 10 °C min^{-1}. The reactor outlet was directly connected to a flame ionization detector. The total amount of adsorbed pyridine was determined by comparing the area of the TPD peaks with the area obtained by calibrated pyridine pulses (1−2 μL) injected to the empty reactor.

Catalysts Preparation. The Pt(0.3 wt %)/$MgAl_2O_4$ catalysts were prepared by incipient impregnation of both supports ($MgAl_2O_4^{cer}$ and $MgAl_2O_4^{cop}$) with an aqueous solution of H_2PtCl_6 at room temperature for 6 h. For the two supports, the Pt concentration in the solution was 2.1 g L^{-1}, and the impregnating volume/support weight ratio was 1.4 mL g^{-1}. In all the cases, a final 0.3 wt % Pt content was obtained. Then the samples were dried at 100 °C for 12 h.

The bimetallic catalysts (PtSn and PtPb) were obtained by impregnation of the corresponding monometallic ones with an aqueous solution of $SnCl_2$ in hydrochloric acid medium or $Pb(NO_3)_2$ at room temperature for 6 h. The Sn contents were 0.3 and 0.5 wt % (concentration of $SnCl_2$ = 2.14 g Sn L^{-1} for 0.3 wt % Sn and 3.57 g Sn L^{-1} for 0.5 wt % Sn; impregnation volume/support weight ratio = 1.4 mL g^{-1}). The contents of Pb were equimolar to those of Sn (equivalent to 0.52 and 0.87 wt % Pb). The impregnation conditions were as follows: concentrations of $Pb(NO_3)_2$ = 3.8 g L^{-1} (0.52 wt % Pb) and 6.2 g L^{-1} (0.87 wt % Pb), and the impregnation volume/support weight ratio = 1.4 mL g^{-1}. After impregnation, the catalysts were dried at 100 °C for 12 h and then calcined under flowing air at 500 °C for 3 h.

Characterization of Catalysts. The characteristics of the metallic phase of catalysts were determined by hydrogen chemisorption, temperature-programmed reduction (TPR), transmission electron microscopy (TEM), X-ray photoelectron spectroscopy (XPS), and test reactions.

H_2 chemisorption measurements were made in a volumetric equipment. The sample weight used was 300−500 mg. The sample was outgassed at room temperature, heated under flowing H_2 (60 mL min^{-1}) from room temperature up to 500 °C, and then kept at this temperature for 2 h. Then, the sample was outgassed under vacuum (10^{-4} Torr) for 2 h. After the sample was cooled down to room temperature (25 °C), hydrogen dosage was performed in the range of 25−100 Torr. The isotherms were linear in the range of used pressures. The chemisorbed hydrogen was calculated by extrapolation of the isotherm to pressure zero. From the data of chemisorbed H_2, the metallic dispersion in monometallic catalysts was calculated by using the formula

$$D = \frac{n_H X M_{Pt}}{W_{cat} C_{Pt}}$$

where n_H = moles of chemisorbed H_2; X = stoichiometry of chemisorbed H_2 on Pt; M_{Pt} = molar mass of Pt; W_{cat} = catalyst weight; and C_{Pt} = Pt content (wt %).

TEM measurements were carried out on a JEOL 100CX microscope with a nominal resolution of 6 Å, operated with an acceleration voltage of 100 kV, and magnification ranges of 80 000× and 100 000×. The samples were prepared by grinding, suspending, and sonicating them in ethanol, and placing a drop of the suspension on a carbon copper grid. After evaporation of the solvent, the specimens were introduced into the microscope column. For each catalyst, a very important number of metallic particles were observed. The mean particle diameter (d) was calculated as

$$d = \frac{\sum n_i \cdot d_i}{\sum n_i}$$

TPR experiments were performed in a quartz flow reactor. The samples were heated at 6 °C min^{-1} from room temperature up to about 600 °C. The reductive mixture (5 v/v % H_2-N_2) was fed to the reactor with a flow rate of 10 mL min^{-1}. Catalysts were previously calcined in situ at 500 °C in air flow for 3 h.

XPS measurements were carried out in a VG-Microtech Multilab spectrometer, which operates with an energy power of 50 eV (radiation Mg Kα, $h\nu$ = 1253.6 eV). The pressure of the analysis chamber was kept at 4×10^{-10} Torr. Samples were previously reduced in situ at 500 °C with H_2 for 2 h. Binding energies (BE) were referred to the C 1s peak at 284.9 eV. The peak areas were determinated by fitting the experimental results with Lorentzian−Gaussian curves.

Cyclohexane dehydrogenation (CHD) and cyclopentane hydrogenolysis (CPH) were carried out in a differential flow reactor. Prior to these reactions, samples were reduced in situ with H_2 at 500 °C. In both reactions the H_2/hydrocarbon molar ratio was 26. The reaction temperature in CHD was 300 °C, whereas in CPH the temperature was 500 °C. The reactor effluent was analyzed by GC.

Butane Dehydrogenation Reaction. The *n*-butane dehydrogenation reaction was carried out in a continuous flow reactor at 530 °C during 2 h. The reactor (with a catalyst weight of 200 mg) was fed with 18 mL min^{-1} of the reactive mixture (*n*-butane + hydrogen, H_2/*n*-C_4H_{10} molar ratio = 1.25). The

reactive mixture was prepared in situ by using mass flow controllers. All gases, *n*-butane, N_2 (used for purge), and H_2 (used for the previous reduction of catalysts and for the reaction) were high-purity ones (>99.99%). Prior to the reaction, catalysts were reduced in situ at 530 °C under flowing H_2 for 3 h. The reactor effluent was analyzed in a GC-FID equipment with a packed chromatographic column (1/8 in. × 6 m, 20% BMEA on Chromosorb P-AW 60/80), which was kept at 50 °C during the analysis. With this analytical device, the amounts of methane, ethane, ethylene, propane, propylene, *n*-butane, 1-butene, cis-2-butene, *trans*-2-butene, and 1,3 butadiene were measured. The *n*-butane conversion was calculated as the sum of the percentages of the chromatographic areas of all the reaction products (except H_2) corrected by the corresponding response factors. The selectivity to a given reaction product (i) was defined as the following ratio: moles of product $i/\sum$ moles of all products (except H_2). Taking into account the high temperatures used for the reaction (for thermodynamic reasons), it was necessary to determine the contribution of the homogeneous reaction. For this purpose, a blank experiment was performed by using a quartz bed and the results showed a negligible *n*-butane conversion (≪1%).

The pulse experiments in *n*-butane dehydrogenation were performed by injecting pulses of pure *n*-butane (0.5 mL STP) into the catalytic bed (100 mg of sample) at 530 °C. The catalytic bed was kept under flowing He (30 mL min^{-1}) between the injections of two successive pulses. Prior to the experiments, all samples were reduced in situ under flowing H_2 at 530 °C for 3 h. The composition of each pulse after the reaction was determined by using a GC-FID equipment with a packed column (Porapack Q). The temperature of the chromatographic column was 30 °C. In these experiments, the *n*-butane conversion was calculated as the difference between the chromatographic area of *n*-butane fed to the reactor and the chromatographic area of nonreacted *n*-butane at the outlet of the reactor, and this difference was referred to the chromatographic area of *n*-butane fed to the reactor. The selectivity to a given product was calculated in the same way than for flow experiments. The carbon amount retained on the catalyst after the injection of each pulse was calculated through a mass balance between the total carbon amount fed to the reactor and the total carbon amount detected by the chromatographic analysis at the outlet of the reactor. The accumulative carbon retention was calculated as the sum of the carbon amount retained after each pulse.

Results and Discussion

The ceramic method involves an addition reaction between γ-Al_2O_3 and MgO. The rate of this reaction depends on the contact area between reactives, the nucleation velocity of the final product, and the diffusion rate of the ions through the phases of reactives and products. These factors are influenced by the particle size, mixing degree, and the structural similarity between the product and, at least, one reactive. Taking into account these considerations, MgO and γ-Al_2O_3 were intimately mixed and ground to a very fine powder using a mortar. With respect to the nucleation velocity of the $MgAl_2O_4$, it must be noted that it is favored due to the structural similarity between the $MgAl_2O_4$ (spinel) and γ-Al_2O_3.[17]

Figure 1 shows XRD results corresponding to the synthesis of $MgAl_2O_4^{cer}$. Figure 1a displays the diffractograms corresponding to the mixture of the reactives (MgO and γ-Al_2O_3). In Figure 1b it can be observed that the main product of the solid-phase reaction was the $MgAl_2O_4$ spinel with remaining amounts of MgO and γ-Al_2O_3. After the purification of the solid

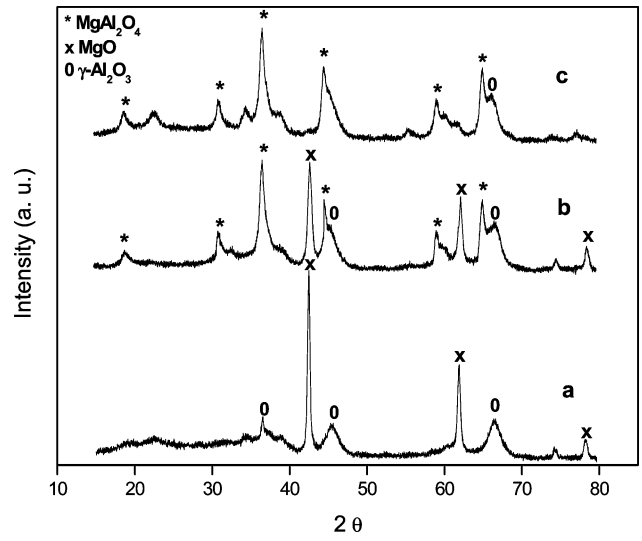

Figure 1. XRD of the mixture of MgO and γ-Al_2O_3, ground with a mortar (a), and $MgAl_2O_4$ obtained by the ceramic method, impurified (b) and purified (c).

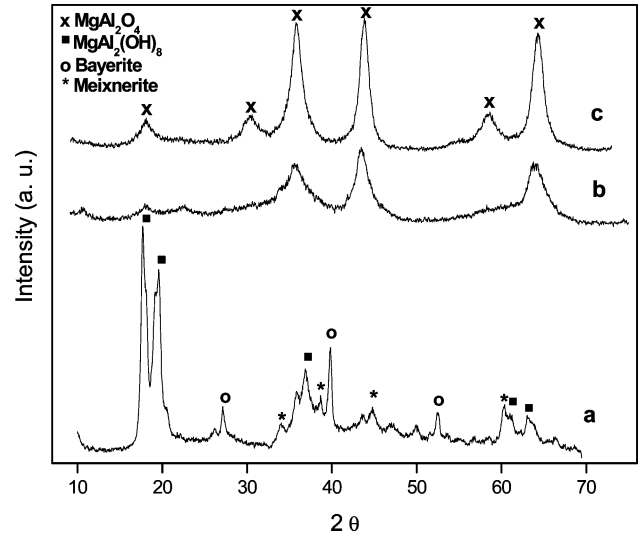

Figure 2. XRD of $MgAl_2O_4$ obtained by coprecipitation method: precursor (a), precursor calcined at 500 °C (b), and precursor calcined at 800 °C (c).

with an aqueous solution of $(NH_4)_2CO_3$ (1 M), DRX experiments show the absence of MgO and the presence of only traces of γ-alumina (Figure 1c). In order to determine the presence of excess of γ-Al_2O_3 in the purified support, a comparison between the cell parameter of the purified spinel and the corresponding to $MgAl_2O_4$ (PDF No. 21-1152) was carried out. Results showed that the content of γ-alumina in the purified support is very small (<1%).

With respect to the coprecipitation method, aluminum and magnesium nitrates were used as reagents and NH_3 as precipitant agent, thus obtaining a precipitated precursor, which is further submitted to a thermal treatment obtaining the $MgAl_2O_4$. Figure 2 shows XRD results that correspond to the synthesis of $MgAl_2O_4$ by the coprecipitation method. Figure 2a displays the diffractogram corresponding to the coprecipitated precursor, thus

Table 1. Textural Properties of Synthesized Supports

support	specific surface (m^2 g^{-1})	pore volume (cm^3 g^{-1})
$MgAl_2O_4^{cer}$	37	0.11
$MgAl_2O_4^{cop}$	108.2	0.33

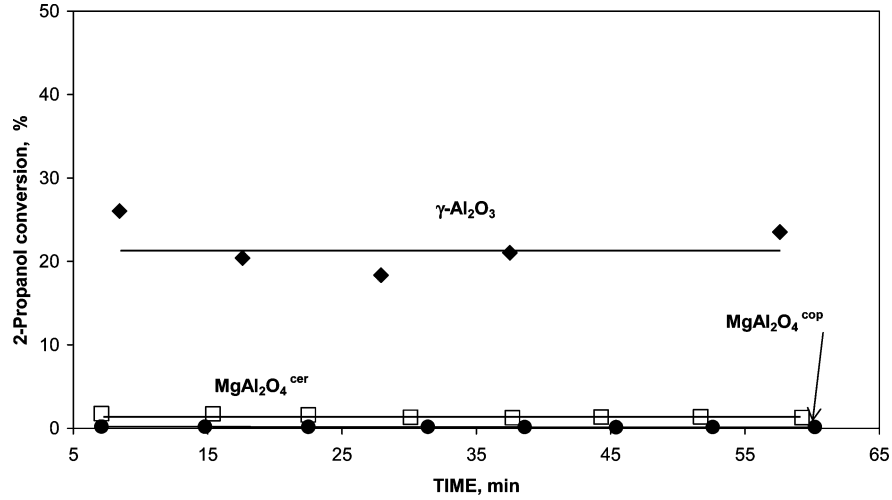

Figure 3. 2-Propanol conversion vs reaction time for γ-Al_2O_3 (reference), $MgAl_2O_4^{cer}$, and $MgAl_2O_4^{cop}$.

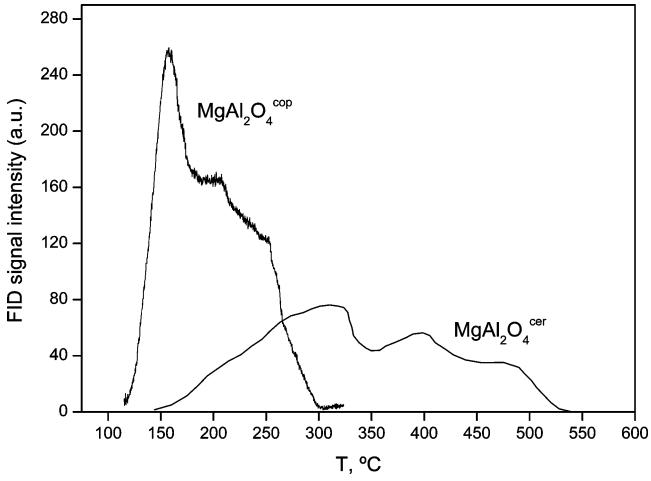

Figure 4. Pyridine TPD profiles of $MgAl_2O_4^{cer}$ and $MgAl_2O_4^{cop}$.

showing that the main phase is a double hydroxide $-MgAl_2(OH)_8-$, together with other double hydroxide, $-Mg_6Al_2(OH)_{18}\cdot 4H_2O$ (meixnerite)−, and $Al(OH)_3$ (bayerite).[3] It can be observed in Figure 2b that, after calcinations of the precursor at 500 °C, some typical peaks of $MgAl_2O_4$ spinel appear. After the calcination at 800 °C, the characteristic peaks of pure $MgAl_2O_4$ spinel are clearly observed in the X-ray diffractogram (Figure 2c).

The textural properties, reported in Table 1, indicate that the support obtained by coprecipitation (with a less severe thermal treatment than that used in the ceramic method) has higher specific surface area and pore volume than the $MgAl_2O_4^{cer}$. These properties of $MgAl_2O_4^{cop}$ would be more suitable for the deposition of the metallic precursor. However, the metal dispersion obtained in the final catalyst also depends on other factors such as the interaction strength between the metallic precursor and the support.

In order to determine the acid properties of the supports, several characterization techniques were used: 2-propanol dehydration reaction, measurements of equilibrium pH, and pyridine desorption experiments. Results of 2-propanol dehydration are shown in Figure 3. It can be observed that γ-Al_2O_3 (reference material), which has Lewis acid centers,[18,19] shows an important activity in the 2-propanol dehydration. On the other hand, both $MgAl_2O_4$ display very low dehydration activities. This means that these materials are practically neutral from the point of view of acid−base properties. However, it must be

Table 2. Hydrogen Chemisorption of Pt, PtSn, and PtPb Catalysts Supported in $MgAl_2O_4$ Synthesized by Both Methods

catalyst	chemisorbed hydrogen (μmol g_{cat}^{-1})	dispersion (%)
$Pt/MgAl_2O_4^{cer}$	3.75	49
$Pt/MgAl_2O_4^{cop}$	2.35	31
$PtSn(0.3)/MgAl_2O_4^{cer}$	1.52	−
$PtSn(0.5)/MgAl_2O_4^{cer}$	1.52	−
$PtSn(0.3)/MgAl_2O_4^{cop}$	1.63	−
$PtSn(0.5)/MgAl_2O_4^{cop}$	1.00	−
$PtPb(0.52)/MgAl_2O_4^{cer}$	0.62	−
$PtPb(0.87)/MgAl_2O_4^{cer}$	0.28	−
$PtPb(0.52)/MgAl_2O_4^{cop}$	1.75	−
$PtPb(0.87)/MgAl_2O_4^{cop}$	1.96	−

Table 3. Initial Rate of Cyclohexane Dehydrogenation Reaction ($R°_{CH}$) and Initial Rate of Cyclopentane Hydrogenolysis ($R°_{CP}$) for Pt, PtSn, and PtPb Catalysts Supported on $MgAl_2O_4$ Synthesized by Both Methods

catalyst	$R°_{CH}$ (mol h^{-1} g_{Pt}^{-1})	$R°_{CP}$ (mol h^{-1} g_{Pt}^{-1})
$Pt/MgAl_2O_4^{cer}$	52.1	7.6
$Pt/MgAl_2O_4^{cop}$	68.1	6.0
$PtSn(0.3)/MgAl_2O_4^{cer}$	20.8	2.0
$PtSn(0.5)/MgAl_2O_4^{cer}$	10.2	2.0
$PtSn(0.3)/MgAl_2O_4^{cop}$	52.7	4.4
$PtSn(0.5)/MgAl_2O_4^{cop}$	40.0	3.6
$PtPb(0.52)/MgAl_2O_4^{cer}$	10.9	1.0
$PtPb(0.87)/MgAl_2O_4^{cer}$	7.0	0.8
$PtPb(0.52)/MgAl_2O_4^{cop}$	40.4	3.5
$PtPb(0.87)/MgAl_2O_4^{cop}$	34.0	2.8

noted that the conversion level of $MgAl_2O_4^{cer}$ in 2-propanol dehydration was slightly higher than that of $MgAl_2O_4^{cop}$. Besides, for both supports the values of equilibrium pH were determined, giving pH values of 8.4 for the $MgAl_2O_4^{cer}$ and 8.6 for the $MgAl_2O_4^{cop}$. Moreover, pyridine desorption experiments (Figure 4) showed low amount of total acid sites in both $MgAl_2O_4$. It must be noted that the total acid sites of a γ-Al_2O_3 (detected by TPD of pyridine) are much higher than those of both spinels. Figure 4 also shows a different distribution of acid sites in both $MgAl_2O_4$. In this sense, $MgAl_2O_4^{cop}$ displays higher amount of weak acid sites since pyridine desorption finishes at low temperature (<300 °C). On the other hand, $MgAl_2O_4^{cer}$ shows mainly sites of medium and strong acidity, since the pyridine is mainly desorbed between 250 and 530 °C. Hence both $MgAl_2O_4$ show very low total acidity and 2-propanol dehydration conversion. The slightly higher dehydration activity displayed by the spinel synthesized by the ceramic method (respect to that prepared by coprecipitation) would be due to

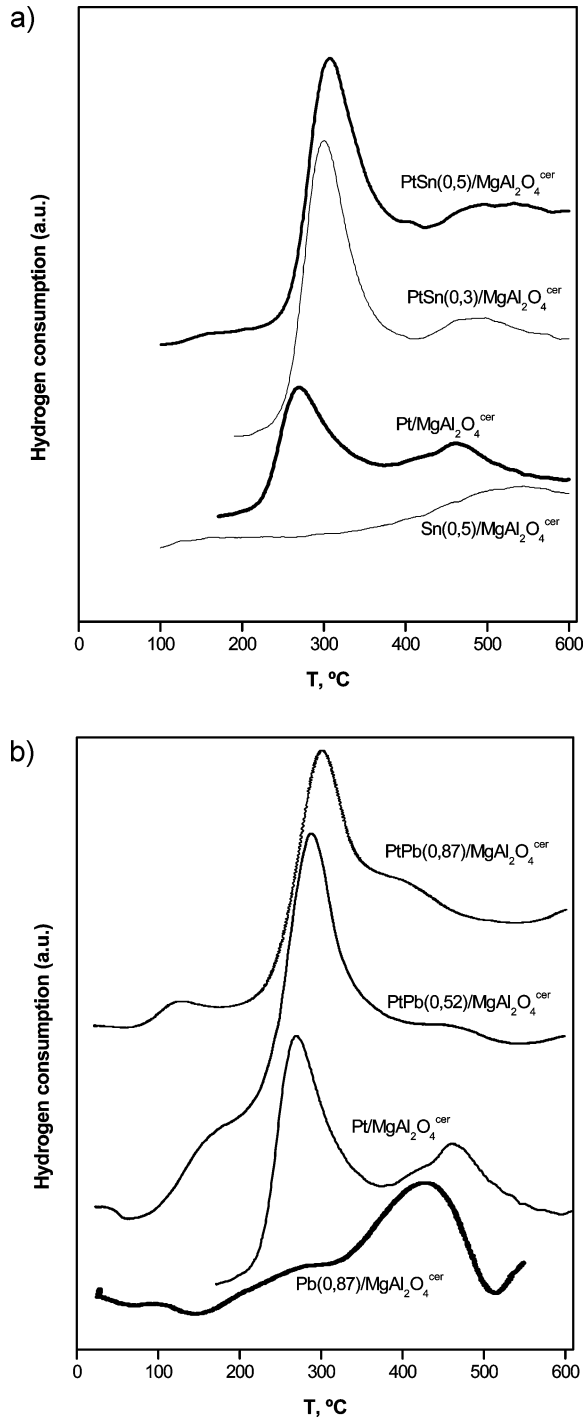

Figure 5. (a) TPR profiles of Pt, Sn, and PtSn catalysts supported on $MgAl_2O_4^{cer}$. (b) TPR profiles of Pt, Pb, and PtPb catalysts supported on $MgAl_2O_4^{cer}$.

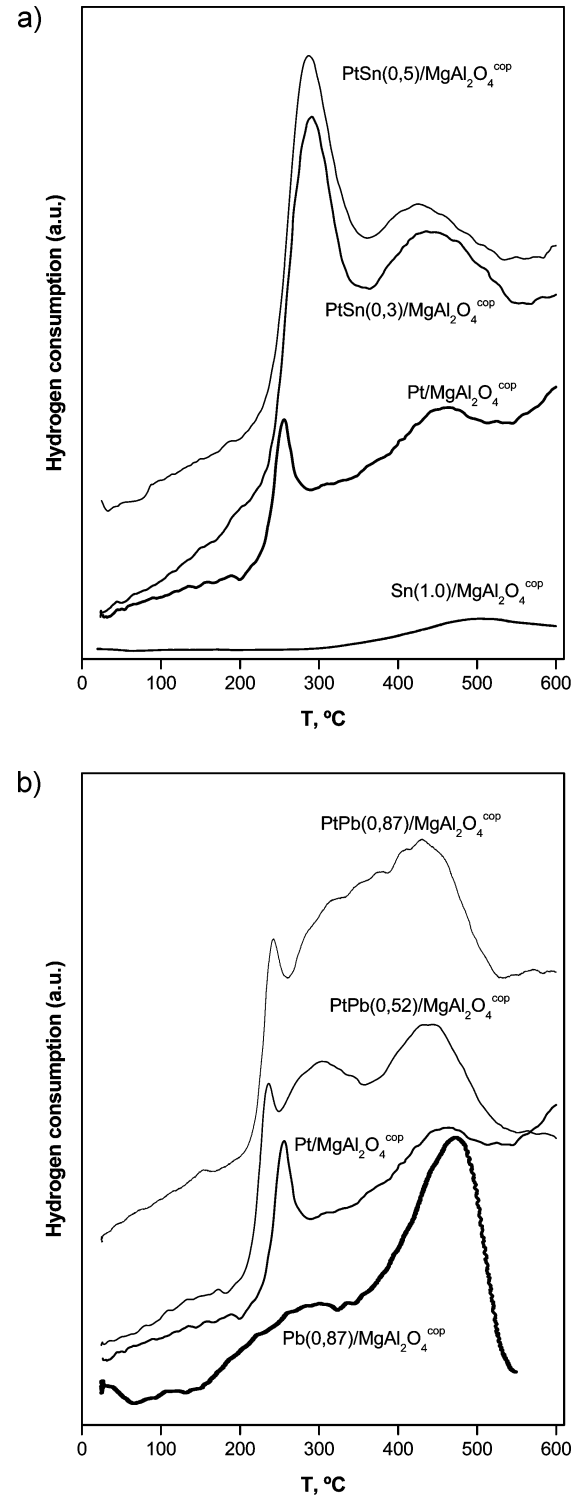

Figure 6. (a) TPR profiles of Pt, Sn, and PtSn catalysts supported on $MgAl_2O_4^{cop}$. (b) TPR profiles of Pt, Pb, and PtPb catalysts supported on $MgAl_2O_4^{cop}$.

the presence of strong acid sites in the first support. In this sense, it was previously reported that the strong acid sites are mainly involved in the propylene formation.[19]

Table 2 displays the H_2 chemisorption results for the different mono- and bimetallic catalysts. It can be observed that the Pt/$MgAl_2O_4^{cop}$ catalyst displays a lower metallic dispersion than the Pt/$MgAl_2O_4^{cer}$ one. In the case of bimetallic catalysts (except for the PtPb/$MgAl_2O_4^{cop}$ catalysts), it is observed that the H_2 chemisorption capacities are clearly lower than those corresponding to the monometallic ones. This effect can be attributed to blocking and/or dilution effects of the Pt by Sn or Pb, and a probable formation of Pt−Sn or Pt−Pb alloys, taking account that both alloys and Sn or Pb do not chemisorb H_2.

The distribution of Pt particle sizes (detected by TEM) corresponding to Pt/$MgAl_2O_4^{cop}$ catalyst shows that the catalyst supported on the $MgAl_2O_4^{cop}$ has Pt particle sizes between 1 and 2 nm (44%), and others between 2 and 3 nm (56%). The mean particle diameter of this catalyst was 1.83 nm. On the other hand, the characterization by TEM of the Pt/$MgAl_2O_4^{cer}$ catalyst showed a lower mean particle diameter (1.32 nm), having Pt particles with sizes between 1 and 2 nm (89%), and

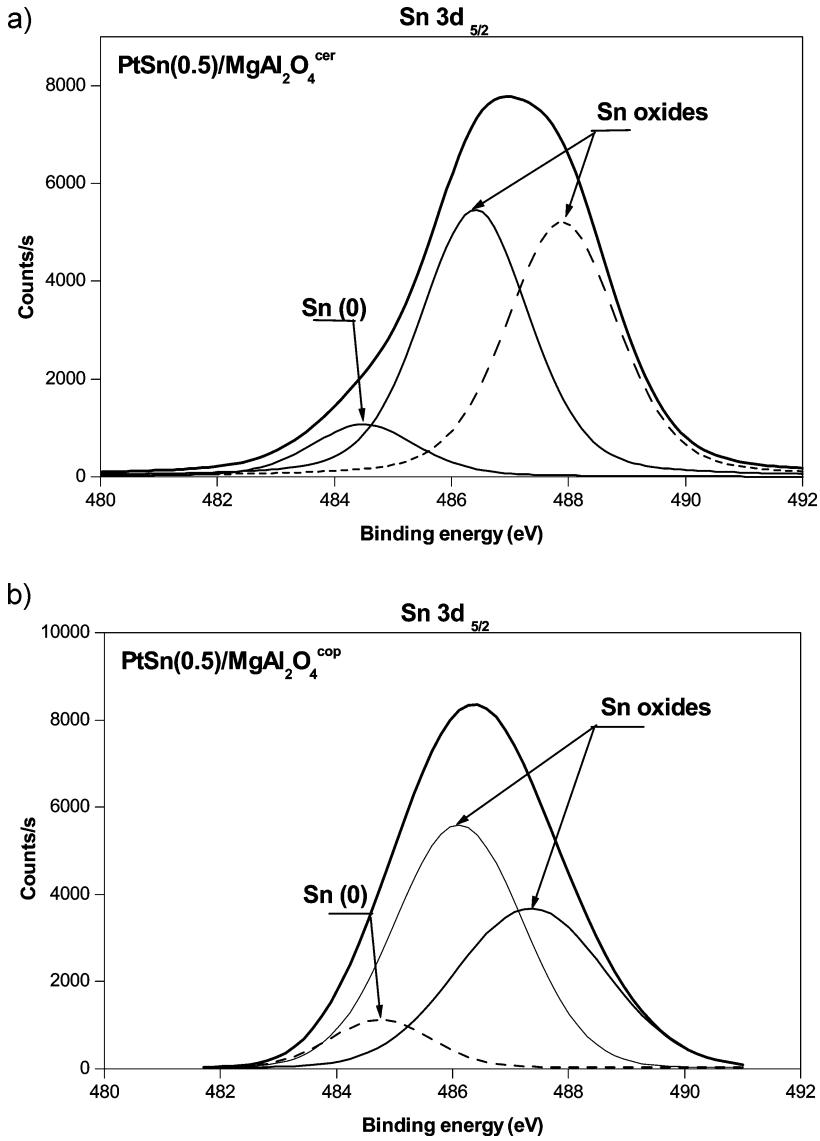

Figure 7. (a) XPS spectrum corresponding to the Sn $3d_{5/2}$ level for PtSn(0.5%)/$MgAl_2O_4^{cer}$ catalyst, previously reduced at 500 °C. (b) XPS spectrum corresponding to the Sn $3d_{5/2}$ level for PtSn(0.5%)/$MgAl_2O_4^{cop}$ catalyst, previously reduced at 500 °C.

others between 2 and 3 nm (only 11%). These results are in agreement with the higher dispersion values obtained for the Pt/$MgAl_2O_4^{cer}$ catalyst by H_2 chemisorption, and they could be related with the higher concentration of strong acid sites on $MgAl_2O_4^{cer}$ observed by isopropanol dehydration and pyridine desorption experiments. Hence during the metallic impregnation, the $MgAl_2O_4^{cer}$ spinel would adsorb anions (like $PtCl_6^{2-}$) with a higher interaction, thus leading probably to a higher metallic dispersion.

Table 3 shows the results obtained in the reaction tests of the metallic phase for mono- and bimetallic catalysts supported on both $MgAl_2O_4$. The cyclohexane dehydrogenation (CHD) is considered a structure-insensitive reaction,[20] and in consequence, the differences in the activities between Pt/$MgAl_2O_4^{cop}$ and Pt/$MgAl_2O_4^{cer}$ catalysts are small to indicate a modification of the active phase between them. The addition of Sn or Pb to Pt (mainly in catalysts supported on the spinel prepared by ceramic method) decreases the initial reaction rate in CHD, though the addition of Pb appears to have a more marked effect on the reaction rate. This fact would be in agreement with results obtained in the literature,[15,21] which indicate that both lead and tin produce blockage of the surface platinum atoms, the first one producing a larger effect than the second one. With respect to the activation energy in this reaction, we observed an increase of the value of 20.7 kcal mol^{-1} for Pt/$MgAl_2O_4^{cer}$ to a value of about 24 kcal mol^{-1} for PtSn/$MgAl_2O_4^{cer}$ catalysts, which would indicate a certain electronic effect in these bimetallic catalysts. On the other hand, this effect is not observed in PtPb/$MgAl_2O_4^{cer}$ catalysts. For catalysts supported in $MgAl_2O_4^{cop}$, the value of activation energy for Pt catalyst is 16.4 kcal mol^{-1} and for the bimetallic PtSn catalysts, the values are close to 16 kcal mol^{-1}. In the same way, the activation energy values for the PtPb/$MgAl_2O_4^{cop}$ catalysts did not increase with respect to the monometallic one.

Table 3 also shows the results of cyclopentane hydrogenolysis (CPH), a structure-sensitive reaction.[22] It can be observed that when Pb and Sn are added to Pt supported in $MgAl_2O_4^{cop}$, there is a decrease of the CPH rate values, this effect being more pronounced for PtPb catalysts. This means that Sn or Pb is intercalated between Pt atoms. On the other hand, when Sn or Pb are added to Pt/$MgAl_2O_4^{cer}$, the decrease of the rate values is more important, and hence the initial reaction rates of CPH are lower than those found for bimetallic catalysts supported on $MgAl_2O_4^{cop}$. These results would indicate higher dilution and blocking effects in bimetallic catalysts supported on

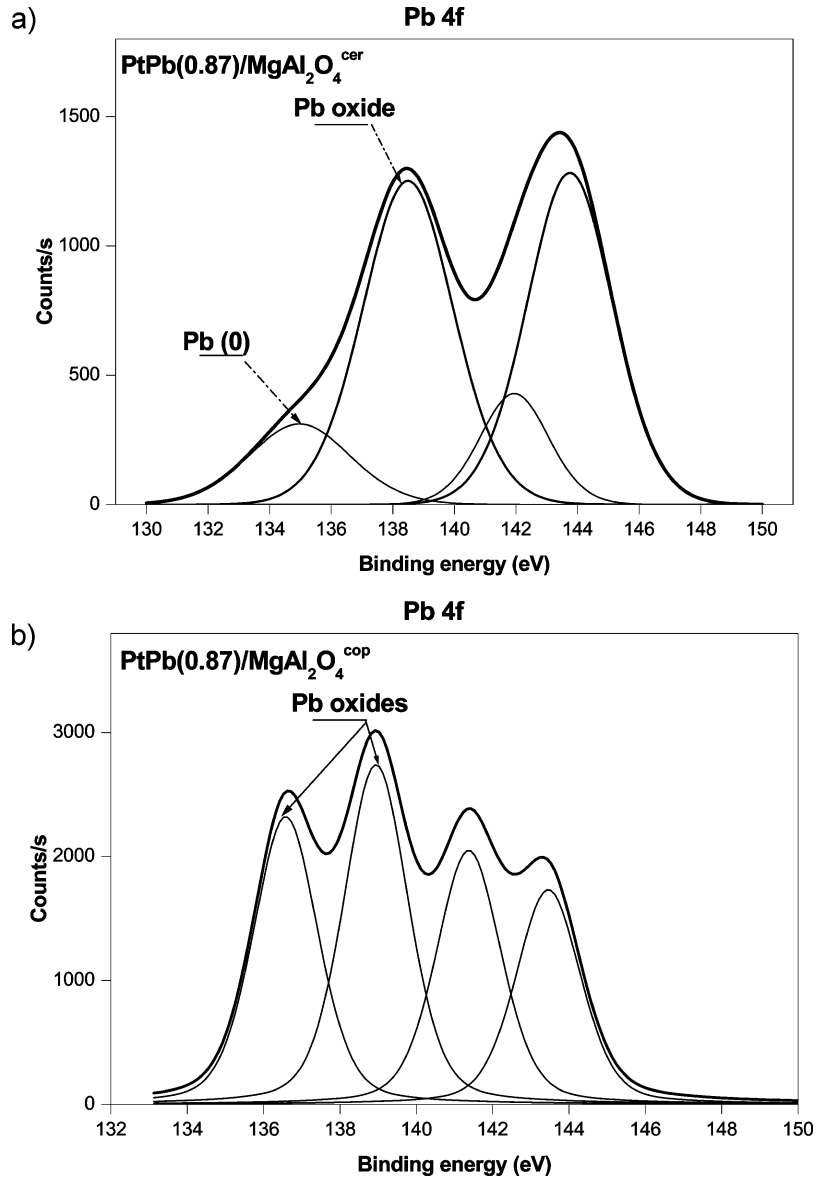

Figure 8. (a) XPS spectrum corresponding to the Pb 4f level for PtPb(0.87%)/$MgAl_2O_4^{cer}$ catalyst, previously reduced at 500 °C. (b) XPS spectrum corresponding to the Pb 4f level for PtPb(0.87%)/$MgAl_2O_4^{cop}$ catalyst, previously reduced at 500 °C.

$MgAl_2O_4^{cer}$. This is in agreement with the H_2 chemisorption capacities and the CHD activities in both catalyst series.

Figures 5 and 6 show the results obtained by temperature-programmed reduction (TPR) on mono- and bimetallic catalysts supported on both $MgAl_2O_4$. It can be observed in Figure 5a,b, for catalysts supported on $MgAl_2O_4^{cer}$, that the Pt/$MgAl_2O_4^{cer}$ has a main reduction peak located at about 270 °C and a broad peak or shoulder at about 450 °C. The presence of two reduction peaks was also observed in Pt/Al_2O_3 catalysts, and it was explained by the existence of two different oxychlorinated Pt species (originated during the impregnation of the support with the chloroplatinic acid).[23] When Sn or Pb is added to Pt, the main reduction peaks are bigger and they are shifted to higher temperatures. Besides, the integrated area of this main reduction peak (in PtSn or PtPb/$MgAl_2O_4^{cer}$) is much higher than that corresponding to the peak of the Pt/$MgAl_2O_4^{cer}$ catalyst. Hence, these results indicate the presence of Pt−Sn or Pt−Pb coreductions. Besides, in both bimetallic catalysts with high Sn or Pb contents, a small shoulder can be observed at about 450−500 °C which can be attributed to reduction of small quantities of isolated species of Sn or Pb. For the Pt catalysts supported on $MgAl_2O_4^{cop}$ (Figure 6a,b), two reduction peaks can be observed, the main one placed at 254 °C, and the secondary one at about 450 °C. The appearance of two reduction peaks is due to different oxychlorinated species of Pt, such as it was previously explained. The main peak is bigger and shifted to higher temperatures when increasing Sn amounts are added to the monometallic catalyst. This behavior could indicate a good interaction between both metals or that a fraction of the second metal would be placed close to Pt. In the case of PtPb catalysts supported on $MgAl_2O_4^{cop}$, the first reduction peak is shifted to slightly lower temperatures than for the monometallic catalyst (Figure 6b), and a broadening of this peak is not observed. Besides, for these catalysts, two reduction zones are found at about 250−350 and 350−500 °C which increase when the Pb amount added to Pt increases. These broad reduction zones are associated to the reduction of free Pb species, since the reduction profile of the Pb/$MgAl_2O_4^{cop}$ catalyst shows two similar reduction zones. These facts would indicate both a Pt−Pb segregation and a low interaction between Pt and Pb.

XPS results of PtSn catalysts supported on both $MgAl_2O_4$ are shown in Figure 7a,b. From the deconvolution of the Sn $3d_{5/2}$ spectra of both PtSn catalysts, three peaks were obtained at 484.4/484.7, 486.1/486.4, and 487.4/487.9 eV, corresponding

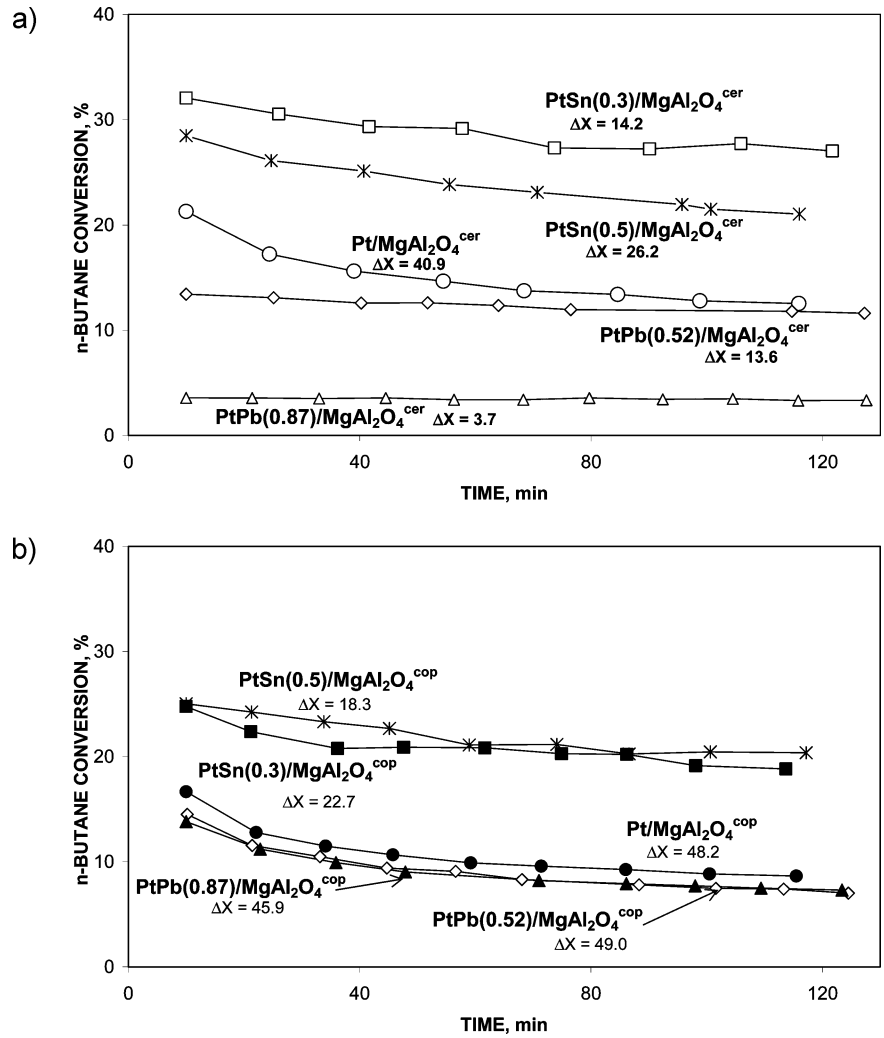

Figure 9. (a) *n*-Butane conversion as a function of reaction time for Pt, PtSn, and PtPb catalysts supported on $MgAl_2O_4^{cer}$. (b) *n*-Butane conversion as a function of reaction time for Pt, PtSn, and PtPb catalysts supported on $MgAl_2O_4^{cop}$.

to different species. It can be observed that the first peak corresponds to a small fraction of Sn (10−15%) in the zerovalent state and probably alloyed with Pt.[24−26] The presence of Sn(0) in bimetallic catalysts and the absence of this species in the Sn monometallic one would indicate a higher Sn reducibility in PtSn catalysts, these results agreeing with TPR ones. The other two peaks are attributed to different oxidized species of Sn.[24−26]

XPS results of PtPb catalysts supported on both $MgAl_2O_4$ are shown in Figure 8a,b. XPS spectra of Pb $4f_{7/2}$ energy levels identify the signal corresponding to Pb(0) and Pb oxides at around 135.5 and 138.5 eV, respectively.[26,27] From the deconvolution of the spectra of PtPb/$MgAl_2O_4^{cer}$ catalysts, Figure 8a shows the presence of Pb(0) species at 134.9 eV together with Pb oxide at 138.6 eV. For the bimetallic catalyst supported on $MgAl_2O_4^{cer}$, the oxidized species (78%) are higher than for metallic Pb (22%). Figure 8b displays (for PtPb/$MgAl_2O_4^{cop}$ catalyst) two peaks placed at 136.7 and 138.9 eV, which would correspond to different Pb oxidized species. In this PtPb/$MgAl_2O_4^{cop}$ catalyst, the absence of metallic Pb is in agreement with TPR results which indicate no interaction between Pt and Pb. On the other hand, in the PtPb/$MgAl_2O_4^{cer}$ catalyst, the presence of Pb(0) indicates a higher interaction between both metals, such as TPR results show.

In conclusion and taking into account the different characterization techniques of the metallic phase, for PtSn catalysts supported on $MgAl_2O_4^{cer}$, tin addition to Pt produces not only important dilution and blocking (geometric) effects but also electronic ones, with probable alloy formation. On the other hand, for PtSn/$MgAl_2O_4^{cop}$ catalyst, there is no electronic interaction between both metals, and thus only geometric effects of the promoter on the active metal predominate. Besides, the effect of Pb addition to platinum is also different according to the preparation method of the $MgAl_2O_4$ spinel. In PtPb/$MgAl_2O_4^{cer}$ catalysts, important geometric effects and a certain PtPb interaction are observed, while in PtPb/$MgAl_2O_4^{cop}$ ones, characterization results show an important segregation between Pb and Pt.

Results of *n*-butane dehydrogenation (flow experiments) are displayed in Figures 9 and 10. The *n*-butane conversion as a function of the reaction time (Figure 9a,b) shows that the initial activity of the Pt/$MgAl_2O_4^{cer}$ catalyst is higher than that of the Pt/$MgAl_2O_4^{cop}$ one, thus agreeing with dispersion measurements obtained by TEM and H_2 chemisorption. Besides, Sn addition to both monometallic catalysts increases the *n*-butane conversion in flow experiments. This increase is more pronounced for catalysts supported on $MgAl_2O_4^{cer}$. On the other hand, the Pb addition to Pt supported on $MgAl_2O_4^{cop}$ slightly decreases the *n*-butane conversion with respect to the corresponding monometallic one, but this decrease in the activity is more pronounced in the case of PtPb catalysts supported on the $MgAl_2O_4$ prepared by the ceramic method. In this last catalyst, the blockage of Pt

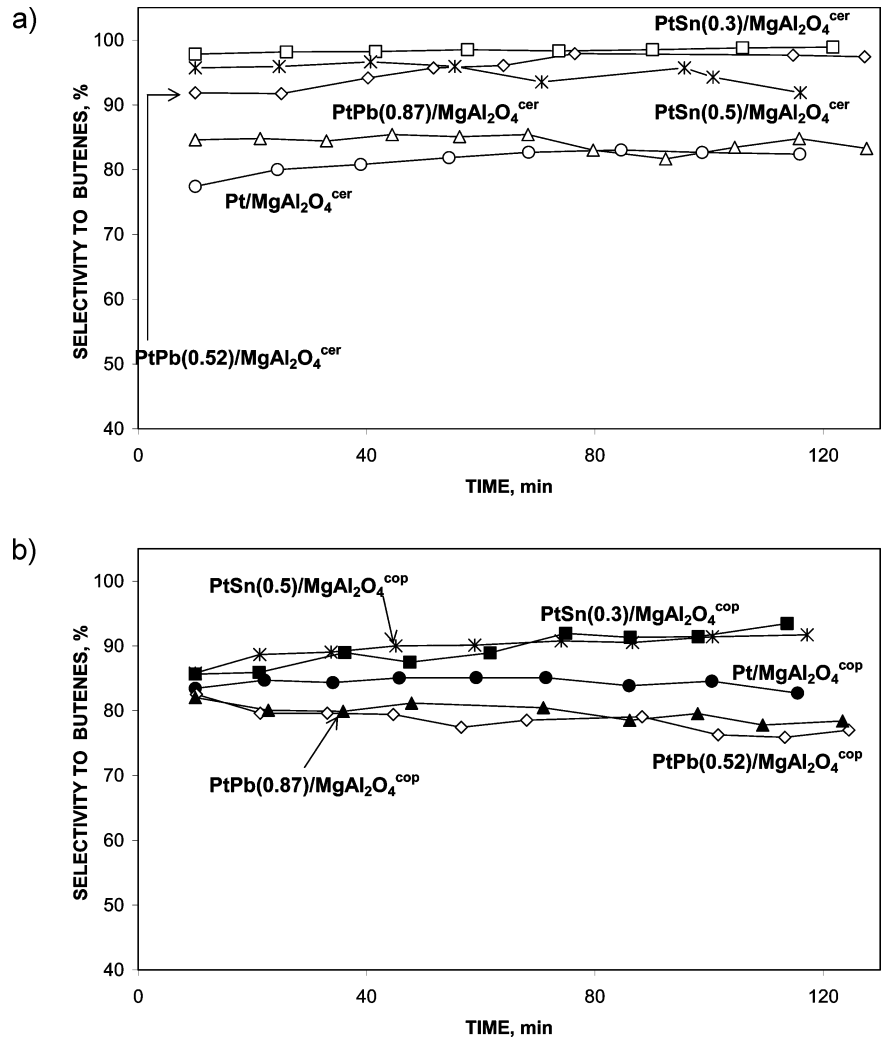

Figure 10. (a) Selectivities to butenes as a function of reaction time Pt, PtSn, and PtPb catalysts supported on $MgAl_2O_4^{cer}$. (b) Selectivities to butenes as a function of reaction time for Pt, PtSn, and PtPb catalysts supported on $MgAl_2O_4^{cop}$.

sites by Pb is very important and produces a poisoning of the metallic phase, decreasing the *n*-butane conversion from 21% for the monometallic catalyst to 3% for the PtPb(0.87)/$MgAl_2O_4^{cer}$ one (Figure 9a).

Besides, the values corresponding to the deactivation parameter (ΔX) along the reaction time, which is defined as $[(X_0 - X_f) \times 100/X_0]$, where X_0 and X_f are the initial and the final conversions, respectively, are also included in Figure 9, a and b. It can be observed that both monometallic Pt catalysts have high deactivation parameters (41−48%). Tin addition to Pt on both supports produces a decrease in the deactivation parameter (ΔX). The lowest value of ΔX (14.2%) corresponds to the bimetallic catalyst with the lower Sn content (0.3 wt %). The ΔX values for PtPb/$MgAl_2O_4^{cer}$ catalysts are low due to the low activities of both samples. On the other hand, the ΔX values for PtPb/$MgAl_2O_4^{cop}$ catalysts are very high (46−49%), similar to that displayed by the corresponding monometallic one (48%). The similarities of the catalytic performances (both in conversion and parameter deactivation) between PtPb/$MgAl_2O_4^{cop}$ catalysts and the corresponding monometallic one are in agreement with TPR results and confirm the important segregation between Pb and Pt when these metals are supported on $MgAl_2O_4^{cop}$.

With respect to the selectivity to all butenes (1-butene, *trans*-2-butene, *cis*-2 butene, and butadiene) shown in Figure 10a,b, Pt/$MgAl_2O_4^{cop}$ catalyst shows a slightly higher selectivity than Pt/$MgAl_2O_4^{cer}$. The Sn addition to Pt/$MgAl_2O_4^{cer}$ (Figure 10a) clearly increases the selectivity to butenes reaching almost 98%. On the other hand, the Pb addition to Pt does not produce an increase of the selectivity to all butenes, except for PtPb(0.52 wt %)/$MgAl_2O_4^{cer}$ catalyst which reaches an initial selectivity value of 90%. The better selectivity of PtPb/$MgAl_2O_4^{cer}$ catalysts could be due to an important blocking effect of Pb on the Pt surface, which decreases the concentration of the large Pt ensembles needed for the undesirable hydrogenolysis reaction.

It must be noted that the best catalytic performance is obtained by the PtSn(0.3 wt %)/$MgAl_2O_4^{cer}$ catalyst. In fact, the initial (32%) and final (28%) conversion values, as well as the initial (98%) and final selectivity values (99%), indicate an excellent behavior in activity, selectivity, and stability of this bimetallic catalyst. In general, it can be seen in Figures 9 and 10 that the ceramic method for the support preparation and the lower Sn content added to Pt lead to better dehydrogenation catalysts. On the contrary, the Pb addition to Pt has a negative effect in the behavior of the catalysts supported in both spinels, mainly in $MgAl_2O_4^{cer}$.

In order to understand the reasons for the better catalytic behavior of some bimetallic catalysts, pulse experiments were carried out to study in more detail the initial steps of the *n*-butane dehydrogenation reaction with respect to the carbon deposition and its relationship with the *n*-butane conversion, the catalyst deactivation, and the selectivity to different products. The carbon retention was calculated by a carbon balance between the inlet

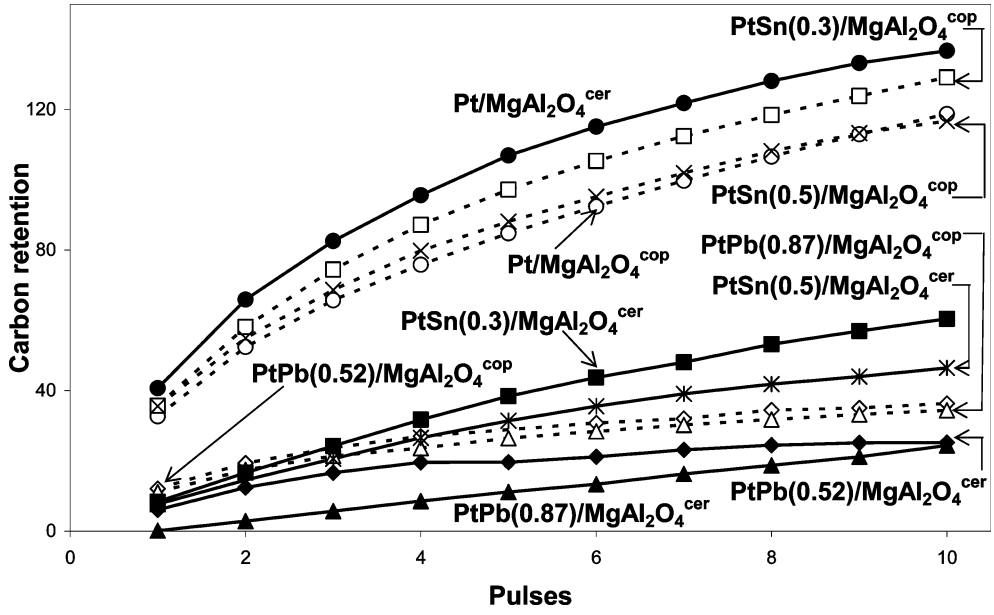

Figure 11. Accumulative carbon retention as a function of the number of *n*-butane pulses injected to Pt, PtSn, and PtPb catalysts supported on $MgAl_2O_4^{cer}$ and $MgAl_2O_4^{cop}$.

and the exit of the reactor. During these experiments, 10 pulses of pure *n*-butane were injected on each sample. It can be observed in Figure 11 that the Sn addition to $Pt/MgAl_2O_4^{cop}$ catalyst does not produce a decrease of the carbon retention with respect to the monometallic one. However, when Sn is added to $Pt/MgAl_2O_4^{cer}$ catalyst, an important decrease of the carbon retention with respect to the monometallic one is observed. All PtPb bimetallic catalysts show low carbon retentions, but this effect can be attributed to the low dehydrogenation activity. The very good catalytic behavior of bimetallic $PtSn/MgAl_2O_4^{cer}$ in activity, stability, and selectivity to butenes in flow experiments is also reflected in the low carbon retention observed in pulse experiments. In this sense, the tin addition to a more dispersed Pt phase (like in $Pt/MgAl_2O_4^{cer}$) would lead to bimetallic PtSn catalysts with a higher intermetallic interaction and hence better catalytic properties than $PtSn/MgAl_2O_4^{cop}$ catalysts. These results agree with characterization ones, where a higher Pt−Sn interaction is observed in $PtSn/MgAl_2O_4^{cer}$ catalysts than in the $PtSn/MgAl_2O_4^{cop}$ ones. On the other hand, the bad catalytic behavior, mainly in activity, of $PtPb/MgAl_2O_4^{cer}$ catalysts is due to the important blocking effect of Pb on the Pt sites, which was observed by the different characterization techniques. With respect to $PtPb/MgAl_2O_4^{cop}$ catalysts, their catalytic activities are slightly lower than that of the corresponding monometallic catalyst due to the presence of important Pt−Pb segregations in these samples.

Conclusions

Both $MgAl_2O_4$ spinels show very low total acidity (measured by 2-propanol dehydration reaction and TPD of pyridine. However, $MgAl_2O_4^{cer}$ displays higher strong acidity than the $MgAl_2O_4^{cop}$ catalyst which seems to influence in the metal−support interaction, since $Pt/MgAl_2O_4^{cer}$ catalyst shows higher metallic dispersion, lower metal particle sizes, and better catalytic behavior than the $Pt/MgAl_2O_4^{cop}$ one.

The Sn addition to monometallic $Pt/MgAl_2O_4$ catalysts improves the performance in the *n*-butane dehydrogenation process, increasing the activity, stability, and selectivity to butenes. This behavior agrees with the catalyst characterization results, where a good Pt−Sn interaction is observed, mainly for bimetallic catalysts supported on $MgAl_2O_4^{cer}$. With respect to PtPb catalysts, the Pb addition to $Pt/MgAl_2O_4^{cer}$ one decreases in an important way the catalytic activity in *n*-butane dehydrogenation, due mainly to the blockage of Pt sites by Pb. On the other hand, in $PtPb/MgAl_2O_4^{cop}$ catalysts, the catalytic activities in *n*-butane dehydrogenation are similar to that of the corresponding monometallic catalyst due to the presence of important Pt−Pb segregations, which were detected by TPR, XPS, and test reactions.

In conclusion, the ceramic method of $MgAl_2O_4$ preparation seems to be the best support for metallic catalysts in the *n*-butane dehydrogenation reaction, and the $PtSn(0.3)/MgAl_2O_4^{cer}$ catalyst was the one that showed the best catalytic performance in this reaction, with *n*-butane conversions higher than 30% and selectivities to butenes very close to 100%.

Acknowledgment

The authors thank Miguel Torres for experimental assistance. Besides, this work was done with the financial support of Universidad Nacional del Litoral and ANPCYT-Argentina.

Literature Cited

(1) Baudin, G.; Martínez, R.; Pena, P. High-temperature Mechanical Behavior of Stoichiometric Magnesium Spinel. *J. Am. Ceram. Soc.* **1995**, *78*, 1857.

(2) Rennard, R.; Freel, J. The Role of Sulfur in Deactivation of $Pt/MgAl_2O_4$ for Propane Dehydrogenation. *J. Catal.* **1986**, *98*, 235.

(3) Armendáriz, H.; Guzmán, A.; Toledo, J.; Llanos, M.; Vazquez, A.; Aguilar-Ríos, G. Isopentane Dehydrogenation on Pt-Sn Catalysts Supported on Al-Mg-O Mixed Oxides: Effect of Al/Mg atomic Ratio. *Appl. Catal., A* **2001**, *211*, 69.

(4) Bocanegra, S. A.; de Miguel, S. R.; Castro, A. A.; Scelza, O. A. n-Butane Dehydrogenation on PtSn Supported on MAl_2O_4 (M: Mg or Zn) Catalysts. *Catal. Lett.* **2004**, *96*, 129.

(5) Guo, J.; Lou, H.; Zhao, H.; Chai, D.; Zheng, X. Dry reforming of Methane Over Nickel Catalysts Supported on Magnesium Aluminate Spinels. *Appl. Catal., A* **2004**, *273*, 75.

(6) Bocanegra, S. A.; Ballarini, A. D.; de Miguel, S. R.; Scelza, O. A. *Mater. Chem. Phys.* **2008**, *111*, 534.

(7) Ye, G.; Troczynski, T. Mechanical Activation of Heterogeneous Sol-gel Precursors for Synthesis of $MgAl_2O_4$ Spinel. *J. Am. Ceram. Soc.* **2005**, *88*, 2970.

(8) Plešingerová, B.; Števulová, N.; Luxová, M.; Boldižárová, E. Mechanochemical Synthesis of Magnesium Aluminate Spinel in Oxide-hydroxide Systems. *J. Mater. Synth. Process.* **2000**, *8*, 287.

(9) Vatcha, S. R.; Trifiro, F.; Cavani, F. *Oxidative Dehydrogenation and Alternative Dehydrogenation Processes—Catalytica Study No. 4992 OD*; Helius, D.; Ed.; Catalytica, Inc.: Mountain View, CA, 1993.

(10) Rioux, R. M.; Komor, R.; Song, H.; Hoefelmeyer, J. D.; Grass, M.; Niesz, K.; Yang, P.; Somorjai, G. A. Kinetics and Mechanism of Ethylene Hydrogenation Poisoned by CO on Silica-supported Monodisperse Pt Nanoparticles. *J. Catal.* **2008**, *254*, 1.

(11) Villegas, J. I.; Kumar, N.; Heikkila, T.; Lehto, V. P.; Salmi, T.; Yu Murzin, D. Isomerization of n-Butane to Isobutane Over Pt-modified Beta and ZSM-5 Zeolite Catalysts: Catalyst Deactivation and Regeneration. *Chem. Eng. J.* **2006**, *120*, 83.

(12) Bocanegra, S. A.; Guerrero-Ruiz, A.; de Miguel, S. R.; Scelza, O. A. Performance of PtSn Catalysts Supported on MAl_2O_4 (M: Mg or Zn) in n-Butane Dehydrogenation: Characterization of the Metallic Phase. *Appl. Catal., A* **2004**, *277*, 11.

(13) Siri, G.; Ramallo-López, J.; Casella, M.; Fierro, J. L. G.; Requejo, F.; Ferretti, O. XPS and EXAFS Study of Supported PtSn Catalysts Obtained by Surface Organometallic Chemistry on Metals: Application to the Isobutane Dehydrogenation. *Appl. Catal., A* **2005**, *278*, 239.

(14) Völter, J.; Lietz, G.; Ulhemann, M.; Hermann, M. Conversion of Cyclohexane and n-Heptane on PtPb-Al_2O_3 and PtSn-Al_2O_3 Bimetallic Catalysts. *J. Catal.* **1981**, *68*, 42.

(15) Palazov, A.; Bonev, C.; Kadinov, G.; Shopov, D.; Lietz, G.; Völter, J. Infrared Spectra of Adsorbed CO and Catalytic Conversion of Cyclohexane on Pt/Al_2O_3 and Pt-Pb/Al_2O_3 Catalysts. *J. Catal.* **1981**, *71*, 1.

(16) Román-Martinez, M. C.; Cazorla-Amorós, D.; Linares-Solano, A.; Salinas-Martinez de Lecea, C.; Yamashita, H.; Anpo, M. Metal-support Interaction in Pt/C Catalysts. Influence of the Support Surface Chemistry and the Metal Precursor. *Carbon* **1995**, *33*, 1.

(17) Domansky, D.; Urretavizcaya, G.; Castro, F.; Gennari, F. Mechanochemical Synthesis of Magnesium Aluminate Spinel Powder at Room Temperature. *J. Am. Ceram. Soc.* **2004**, *87*, 2020.

(18) Pines, H.; Haag, W. Alumina: catalyst and support: I. Alumina, its intrinsic acidity and catalytic activity. *J. Am. Chem. Soc.* **1960**, *82*, 2471.

(19) García Cortez, G.; de Miguel, S.; Scelza, O.; Castro, A. Study of the poisoning of Al_2O_3 by alkali metals addition. *J. Chem. Technol. Biotechnol.* **1992**, *53*, 177.

(20) Cinneide, A. D.; Clarke, J. K. A. Catalysis on Supported Metals. *Catal. Rev.* **1972**, *7*, 213.

(21) Cheung, T. T. P. X-ray photoemission studies of Pt-Sn and Pt-Pb bimetallic systems. *Surf. Sci.* **1986**, *177*, 493.

(22) Boudart, M. Catalysis by supported metals. *Adv. Catal.* **1969**, *20*, 153.

(23) Lietz, G.; Lieske, H.; Spindler, H.; Hanke, W.; Völter, J. Reactions of platinum in oxygen- and hydrogen-treated Pt γ-Al_2O_3 catalysts. II. Ultraviolet-visible studies, sintering of platinum, and soluble platinum. *J. Catal.* **1983**, *81*, 17.

(24) Llorca, J; Ramírez de la Piscina, P.; Riera, M.; Fierro, J. L. G.; Sales, J.; Homs, N. *J. Mol. Catal. A* **1997**, *118*, 101.

(25) Homs, N.; Llorca, J.; Riera, M.; Jolis, J.; Fierro, J. L. G.; Sales, J.; Ramírez de la Piscina, P. Silica-supported PtSn alloy doped with Ga, In or, Tl: characterization and catalytic behaviour in n-hexane dehydrogenation. *J. Mol. Catal. A* **2003**, *200*, 251.

(26) Wagner, C. D.; Riggs, W. M.; Davis, L. E.; Moulder, J. F. *Handbook of X-ray Photoelectron Spectroscopy*; Perkin-Elmer Corp.: Waltham, MA, 1993.

(27) Del Angel, G.; Torres, G.; Bertin, V.; Gómez, R.; Morán-Pineda, M.; Castillo, S.; Fierro, J. L. G. The role of lanthanum oxide in the formation of NO_2 over Pt-Pb/Al_2O_3-La_2O_3 catalysts under lean-burn conditions. *Catal.Commun.* **2006**, *7*, 232.

Received for review June 4, 2009
Revised manuscript received August 27, 2009
Accepted March 13, 2010

IE9009205